

# Dendrites of Mammalian Neurons Contain Specialized P-Body-Like Structures That Respond to Neuronal Activation

Nicolas Cougot,<sup>1\*</sup> Suendra N. Bhattacharyya,<sup>2\*</sup> Lucie Tapia-Arancibia,<sup>3,4</sup> Remy Bordonné,<sup>1</sup> Witold Filipowicz,<sup>2</sup> Edouard Bertrand,<sup>1</sup> and Florence Rage<sup>1</sup>

<sup>1</sup>Institut de Génétique moléculaire de Montpellier, Centre National de la Recherche Scientifique Unité Mixte de Recherche 5535-IFR 122, 34000 Montpellier, France, <sup>2</sup>Friedrich Miescher Institute for Biomedical Research, 4002 Basel, Switzerland, <sup>3</sup>INSERM U710, Université de Montpellier 2, Montpellier, F-34095 France, and <sup>4</sup>Ecole de Hautes Etudes Pratiques, Paris, F-75007 France

Intracellular mRNA transport and local translation play a key role in neuronal physiology. Translationally repressed mRNAs are transported as a part of ribonucleoprotein (RNP) particles to distant dendritic sites, but the properties of different RNP particles and mechanisms of their repression and transport remain largely unknown. Here, we describe a new class of RNP-particles, the dendritic P-body-like structures (dLPbodies), which are present in the soma and dendrites of mammalian neurons and have both similarities and differences to P-bodies of non-neuronal cells. These structures stain positively for a number of P-body and microRNP components, a microRNA-repressed mRNA and some translational repressors. They appear more heterogeneous than P-bodies of HeLa cells, and they rarely contain the exonuclease Xrn1 but are positive for rRNA. These particles show motorized movements along dendrites and relocate to distant sites in response to synaptic activation. Furthermore, Dcp1a is stably associated with dLP-bodies in unstimulated cells, but exchanges rapidly on neuronal activation, concomitantly with the loss of Ago2 from dLP-bodies. Thus, dLP-bodies may regulate local translation by storing repressed mRNPs in unstimulated cells, and releasing them on synaptic activation.

**Key words:** miRNA; P-body; RNA-granule; neurons; dendritic mRNA trafficking; localization

## Introduction

In neurons, local mRNA translation is important to ensure the compartmentalized protein expression required for synaptic plasticity (Klann and Dever, 2004; Fuchs et al., 2006; Sutton and Schuman, 2006; Twiss and van Minnen, 2006). Messenger RNAs are trafficked to dendritic translation sites as parts of ribonucleoprotein complexes, which remain translationally dormant until they reach their destination (Krichevsky and Kosik, 2001; Kindler et al., 2005). Several studies have shown that RNA and RNA-binding proteins undergo motorized transport along axons and dendrites. Interestingly, this frequently involves the formation of large molecular complexes, which are visible microscopically as

granules (Hirokawa, 2006; Kiebler and Bassell, 2006). For instance, a zipcode binding protein, ZBP1 (IMP1), which binds  $\beta$ -actin mRNA (Ross et al., 1997), is part of motile granules in dendrites of hippocampal neurons (Zhang et al., 2001) and in *Xenopus* growth cones (Deshler et al., 1998; Havin et al., 1998). Similarly, survival of motor neuron (SMN) and fragile mental retardation proteins (FMRP) localize in foci that show motorized movement along dendrites (Zalfa et al., 2006).

MicroRNAs (miRNAs) are a class of ~21-nt-long, noncoding RNAs that can reversibly repress translation of target mRNAs (Pillai et al., 2007). This property makes them good candidates for factors regulating local mRNA translation. Dozens of different miRNAs have been identified in neuronal vertebrate cells (Sutton and Schuman, 2006), and a brain specific miRNA has recently been shown to accumulate in dendrites and to regulate dendritic spine development by controlling local expression of protein kinase LIMK1 (Lagos-Quintana et al., 2002; Krichevsky et al., 2003; Schrott et al., 2006). Interestingly, components of miRNA machinery such as argonaute (Ago) proteins and miRNAs, and mRNAs repressed by miRNAs are enriched in evolutionary conserved cytoplasmic structures called P-bodies (also termed Dcp or GW bodies), which function as sites of both mRNA degradation (Cougot et al., 2004), and storage of translationally repressed mRNAs (Liu et al., 2005; Pillai et al., 2005; Bhattacharyya et al., 2006). The markers most frequently used to visualize P-bodies are components of the decapping complex, Dcp1a and Dcp2, decapping activators (e.g., RCK/p54), the 5'-3' exonuclease Xrn1, and GW182, which is involved in the miRNA

Received Sept. 1, 2008; revised Oct. 14, 2008; accepted Oct. 24, 2008.

This work was supported by grants from Agence Nationale de la Recherche, France (ANR-05-BLAN-0118-01) and La Ligue contre le Cancer. Research by S.N.B. and W.F. was partially supported by EC FP6 Program "Sirocco." Friedrich Miescher Institute is a part of Novartis Research Foundation. S.N.B. is a former recipient of an International Human Frontier Science Program organization (HFSP) long-term fellowship and is currently holding an HFSP Career Development Award at Indian Institute of Chemical Biology (IICB). N.C. has a fellowship from L'Association pour la Recherche contre le Cancer. We thank Montpellier RIO Imaging for their assistance. We thank A. Matus and H. Brinkhaus of the Friedrich Miescher Institute for providing us with -cultured rat hippocampal neurons. We also thank T. Hobman, R. Pillai, C. Artus-Revel, J. Lykke-Andersen, R. Willemsen, B. Séraphin, M. J. Fritzer, J. Steitz, and R. Singer for providing plasmids and/or antibodies, Michel Vignes for glutamatergic agonist and antagonist, and M. Kiebler for valuable discussion.

\*N.C. and S.N.B. contributed equally to this work.

Correspondence should be addressed to Florence Rage, Institut de Génétique moléculaire de Montpellier, 1919 route de Mende 34000 Montpellier, France. E-mail: florence.rage@igmm.cnrs.fr.

S. N. Bhattacharyya's present address: Indian Institute of Chemical Biology, 4, Raja SC Mullick Road, Kolkata 700032, India.

DOI:10.1523/JNEUROSCI.4155-08.2008

Copyright © 2008 Society for Neuroscience 0270-6474/08/2813793-12\$15.00/0

pathway. In addition, P-bodies also contain many other factors involved in mRNA metabolism and regulation of translation (Eulalio et al., 2007). A recent study has shown that, in *Drosophila*, neuronal processes contain structures related to P-bodies. These granules contain dStaufen and dFMRP and share many components with somatic P-bodies (Barbee et al., 2006), raising the possibility that some previously characterized RNA granules represent a specialized class of P-bodies, adapted to neuronal function.

P-bodies in mammalian neurons have not been characterized. It is not known whether they are restricted to the soma, or whether they are also present in dendrites or axons. Furthermore, the relationship between P-bodies and previously described neuronal RNA granules is unknown, and the possibility that neuronal P-bodies could be involved in mRNP transport and storage has not been explored. Here, we demonstrate that P-body-like structures are present in the soma and dendrites of mammalian neurons and have both similarities and differences to P-bodies of non-neuronal cells.

## Materials and Methods

**Primary cultures of rat neurons.** Primary cultures of rat hypothalamic neurons were prepared by mechano-enzymatic dissociation of fetal Sprague Dawley rat hypothalamus (day 17), as described previously (Rage et al., 1999). Briefly, cells were grown during 8–10 d, at which time they reach maturity and make well established and stable synapses (Scarborough et al., 1989). Neuronal cultures from E19 rat hippocampus were prepared and maintained in culture on glass coverslips for 3 weeks according to the methods described previously (Fischer et al., 1998).

**Plasmid constructs.** Plasmids allowing expression of GFP-Dcp1a (van Dijk et al., 2002), YFP-ZBP1 (Eom et al., 2003), GFP-FMRP (Tiruchinappalli et al., 2003), and plasmids encoding Renilla luciferase reporters RL-3xB and RL-3xBMut (Pillai et al., 2005), were previously described. Ago2-GFP and SMN-RFP were constructed with the Gateway cloning strategy (Invitrogen). Details of plasmid construction are available on request.

**Transfections.** Primary hypothalamic neurons were transfected with calcium phosphate plasmid DNA precipitate, according to the published protocol (Xia et al., 1996). Briefly, cells were placed in a transfection medium containing DMEM, DMKY (0.5% phenol red, 1 M HEPES, 10 mM MgCl<sub>2</sub>), received the preformed calcium phosphate plasmid DNA precipitate, and were incubated for 45 min. The medium was then removed and cells were washed with HBS for 1 min. Preconditioned medium, removed from the culture before the transfection, was reintroduced and cells were continued in culture for 24 additional hours. For hypothalamic neurons, 2–3 μg of plasmid DNA were used per 35 mm dishes.

HeLa cells were transfected using Lipofectamine Plus reagent or Lipofectamine 2000 (Invitrogen) according to manufacturer's protocol. 100–200 ng of plasmid DNA per well of a 6 well tissue culture plate was used for each transfection and cells were analyzed 48 h after transfection.

For drug treatment, hypothalamic neurons were cultivated for 8 d *in vitro*, and cells were incubated with different glutamatergic receptor agonists [NMDA (30 μM), kainate (50 μM) or DHPG (50 μM)], or BDNF (50 mg/ml) and KCl (50 mM) for 15 min, 30 min or 1 h. When indicated, specific antagonists of NMDA and kainate, MK801 (10 μM) and DNQX (50 μM), respectively, were added to the culture medium 10 min before agonist treatment.

**Immunofluorescence and *in situ* hybridization.** For immunofluorescence analysis, neurons were fixed with prewarmed 4% paraformaldehyde and 3% sucrose in PBS for 10 min at room temperature. Cells were permeabilized in 0.2% Triton X-100 in 1 × PBS for 10 min and blocked in PBS containing 1% BSA and 5% normal goat serum for 1 h at room temperature. Neurons were incubated with the primary antibodies in the blocking buffer at 4°C overnight. Secondary antibodies were labeled with Alexa 488 or Alexa 594 and were used at 1:500 dilution. Rabbit polyclonal anti-Dcp1 serum (kindly provided by B. Séraphin, CNRS, Gif-sur-Yvette), raised against a recombinant human Dcp1a, was used at 1:4000

dilution. Mouse monoclonal anti-Dcp1a was purchased from Abcam. Goat anti-PSD95 antibody (Santa Cruz), and rabbit anti-Ago2 (a kind gift from T. Hobman, University of Alberta, Edmonton, Alberta, Canada), raised against a recombinant rat Ago2 protein fragment, were used at 1:100 dilution. Note that anti-Ago2 antibody detects all four mammalian Ago proteins. Rabbit anti-RCK/p54 (Bethyl Laboratory), anti-rRNA monoclonal Y10B (obtained from J. Steitz, Yale University Medical School, New Haven, CT), and anti-ZBP1 antibodies (obtained from the laboratory of R. H. Singer, Albert Einstein College of Medicine, NY) were used in 1:500 dilutions. The autoimmune serum against human GW182 protein (18033; a gift from M. J. Fritzler, University of Calgary, Calgary, Alberta, Canada) was used for detection of GW182. Anti-TAU1 antibody was a kind gift from V. Homburger, IGF, Montpellier, France.

For *in situ* analysis of neurons, slide preparation, hybridization and washing were done as described previously (Pillai et al., 2005). The miR-CURY LNA probe used for the *in situ* detection of miR-128 or let-7 miRNA were purchased from Exiqon (Vedbaek, Denmark) and labeled with digoxigenin, using the terminal transferase 3'-DIG-tailing kit (Roche Biochemicals). The anti GW182 serum was used as the source of primary antibody against GW182 to stain the P-body-like structures. Alexa 488 fluorochrome labeled goat-anti human antibody (1:500; to detect the GW182 signal) was used in combination with the Fluorescent Antibody Enhancer Set for DIG Detection (Roche Biochemicals) to detect the signals for the miRNAs.

**Preparation of synaptosomes, immunoprecipitation, and Western and Northern blot analyses.** Synaptosomes from brain extracts of adult male BALB/C6 mice were prepared essentially as described previously (Bagni et al., 2000). A brain homogenate was prepared in a homogenization buffer [20 mM HEPES-KOH pH 7.5, containing 320 mM sucrose, 0.25 mM EDTA, 30 U/ml Nsain and 1 × protease inhibitor mix without EDTA (Roche)]. The homogenate was precleared by centrifugation at 1000 × g and then centrifuged at 14,000 × g to collect crude synaptosomes. The pellet was resuspended in the homogenization buffer and further purified on a Percoll step gradient (2, 6, 10 and 20% Percoll concentration), and by flotation on a discontinuous Optiprep gradient (9, 12.5, 15, 25 and 35%), all prepared in the homogenization buffer. The purified synaptosome fraction was stored at -70°C in the homogenization buffer containing 50% glycerol. For protein analysis, synaptosomes were extracted with an equal volume of 2 × IP buffer (20 mM Tris-HCl, pH 7.5, 10 mM MgCl<sub>2</sub>, 400 mM KCl, and 1% Triton X-100) for 15 min on ice. The extract was clarified by centrifugation at 14,000 × g for 5 min at 4°C and the supernatant used for immunoprecipitation analysis. Anti-RCK/p54 and anti-ZBP1 antibodies, described above, were cross-linked to Protein G Sepharose beads and 25 μl of cross-linked beads (500 ng of proteins) were incubated with a supernatant prepared from 1 mg of purified synaptosomes, in 1 ml reaction at 4°C overnight. After washing, the beads were extracted with SDS-solubilizing buffer and analyzed on a 10% SDS-PAGE followed by Western blotting, using anti-ZBP1 (1:1000) and anti-RCK/p54 (1:10,000) antibodies.

For Western analysis, 100 μg of total protein from each synaptosome purification step was resolved on 10% SDS-PAGE, followed by Western blotting using anti-Ago2 (1:1000) and anti-PSD95 (1:500) antibodies. For Northern blot analysis, 10 μg of total RNA extracted from each fraction was resolved on 15% 7 M urea-PAGE, electrotransferred to Nybond N<sup>+</sup> membrane, and hybridized with <sup>32</sup>P-labeled oligodeoxynucleotide complementary to miR-128.

**Live cell imaging.** For live cell analysis, we used a wide-field Nikon TE200 (100× objective, NA 1.45), equipped with an EM-CCD camera (Cascade 512B, Roper). For FRAP, z-stacks were captured every 3 s with a piezzo motor. For image analysis, fluorescence intensities were measured as described by Boireau et al. (2007). Briefly, a small parallelepiped (1 × 1 × 1.5 μm) was placed at the most intense area of the region in which the foci resided. This operation was done automatically by a macro that was created in ImageJ. This automatic tracking of foci in three dimensions (3D) allowed to correct cell movements and to minimize signal from diffusing proteins. The validity of the tracking procedure was verified by eye. Signal was then subtracted from background and normalized to prebleached values. For time-lapse, z-stacks were captured every

200–250 ms during 5–10 s. Movies were then assembled after projection of z-stacks using MetaMorph.

**Image acquisition and processing.** Images were acquired on a DMRA microscope equipped for epifluorescence, and with a 100× PlanApo objective and a 1.6× eyepiece. Digital images were recorded with a 12-bit C4795-NR CCD camera (Hamamatsu). Both the camera and the microscope were controlled by the software MetaMorph. Three-dimensional images were deconvolved with the software Huygens 2.3 (Scientific Volume Imaging b.v.), using a MLE algorithm. Maximal image projections of the resulting stacks were then converted to 8-bit images and colorized with PhotoShop (Adobe).

Pictures representing neurons over long distances were reconstructed from three pictures taken with 100× objective and assembled with MRI Cell Image Analyzer (Volker Bäcker). To define the border of neurons, we used the weak and diffuse cellular autofluorescence in immunofluorescence experiments, and the diffuse GFP signal in transfected cells. Distances of different granules along the dendrites were measured using NeuronJ software (<http://www.mri.cnrs.fr/index.php?m=38>) (Meijering et al., 2004). For experiments done in Friedrich Miescher institute, images were taken with a Zeiss Imager Z1 microscope equipped with Zeiss Plan-APOCHromat 100× or 40× lens and AxioCam MRM T2-C1.0X monochrome camera. For taking DIC images, a filter adapter PA HC 100X/1.40 II was used. The images were processed either with Axio-Vision Rel.4.5 or Imaris software, and mounted in Adobe Photoshop CS2.

For the quantitative analysis of the colocalization of foci labeled by the different proteins, we used the Spot function of Imaris (Bitplane), which allowed us to consider only the signal present in foci. This software first applies a Gaussian filter of a given size (0.3 μm in this case) to remove small objects, and then identifies local maxima above a given threshold (the same threshold was used all images of a given data set). Eye-examination verified that this procedure correctly identified dIP-bodies and other foci present in cells. To quantify colocalization between foci, the Spot function was run in each channel, and the spots that colocalized or did not colocalize were then counted. Although the numbers calculated were similar to those found by eye-examination, this ensured an unbiased analysis of the images. Each colocalization analysis was performed on a total of 6–10 cells representing 60–125 spots. Concerning Xrn1, we compared the localization of Dcp1a foci that had a similar intensity in the soma and dendrites. This ensured that the lack of detection of Xrn1 in dendritic P-bodies was not caused by a low intensity of the signals.

## Results

### P-body components are enriched in dendritic foci in rat hippocampal and hypothalamic neurons

Localization of selected P-body components, Dcp1a, GW182, RCK/p54, and Ago proteins, was analyzed in primary cultures of rat hippocampal and hypothalamic neurons. In hippocampal neurons labeled with anti-GW182 antibodies, the signal was concentrated in foci (Fig. 1A), and double-labeling experiments with anti-Dcp1a, anti-RCK/p54 and anti-Ago2, revealed that most of the GW182 foci contain these proteins (supplemental Figs. S1, S2, and S3, available at [www.jneurosci.org](http://www.jneurosci.org) as supplemental material). However, not all foci were doubly labeled, indicating that their composition tolerated some heterogeneity. Likewise, in hypothalamic neurons labeled with anti-Dcp1a antibodies, the signal appeared in foci, and many of them were also labeled with anti-Ago2 and anti-RCK/p54 antibodies (Fig. 1B,D). Again, the foci did not match perfectly, and in particular, a fraction of Ago2 foci did not contain Dcp1a. To quantify the degree of colocalization between these proteins, we used first Dcp1a as a reference and counted the number of Dcp1a foci that contained GW182, Ago2 or RCK/p54. We then performed the reciprocal analysis by using foci labeled by GW182, Ago2 or RCK/p54 as references, and counting the fraction that contained Dcp1a. The results, shown in supplemental Figure S4 (available at [www.jneurosci.org](http://www.jneurosci.org) as supplemental material), showed that Dcp1a, GW182 and RCK/p54 all colocalized together with a high frequency (>65%). Dcp1a foci also

contained Ago2 nearly all the time, but Ago2 frequently formed additional foci that did not contain detectable Dcp1a (60% of Ago2 foci).

To determine whether the foci were in dendrites, axons, or both, we labeled hypothalamic neurons for Dcp1a and either MAP2, a dendritic marker, or TAU1, an axonal protein. Dcp1a foci were present in dendrites (Fig. 1C), but appeared excluded from axons (supplemental Fig. S5A, available at [www.jneurosci.org](http://www.jneurosci.org) as supplemental material). Next, we assessed whether the foci were present in postsynaptic compartments. In hippocampal neurons, costaining for the postsynaptic density protein PSD95 revealed that a small fraction of GW182 foci accumulated in the vicinity of dendritic spines (Fig. 1A), and this was further supported by colabeling with TRITC-phalloidin, which stains the polymerized actin in dendritic spine heads (supplemental Fig. S5B, available at [www.jneurosci.org](http://www.jneurosci.org) as supplemental material). Synaptic localization of some P-body components was also confirmed by a biochemical approach. Purified synaptoneurosome, enriched in postsynaptic density protein marker PSD95, were found to contain Dcp1a (Fig. 1E).

Thus, our results indicate that in hippocampal and hypothalamic neurons, P-body-like structures are present in dendrites, sometimes in proximity of synapses. These structures contain Dcp1a, GW182, RCK/p54 and Ago2, but they appear to have some degree of heterogeneity as the foci labeled by these proteins did not perfectly overlap. Because the vast majority of the foci labeled by anti-Dcp1a or anti-GW182 antibodies colocalized with each other, we chose to use GW182 and Dcp1a as references in the subsequent series of experiments, and we referred to the structures they label as dIP-bodies (dendritic P-body-like structures).

### Neuronal dIP-bodies contain miRNAs and a repressed mRNA target

Because dIP-bodies were found to contain Ago2, a component of miRNPs, we also assessed the localization of miRNAs. Let-7 miRNA is highly expressed in brain, and *in situ* hybridization indicated that it was present in dIP-bodies as indicated by its colocalization with GW182 (Fig. 2A). The mutant let-7 probe (Pillai et al., 2005), used as a control, did not stain the GW182 foci (supplemental Fig. S6A, available at [www.jneurosci.org](http://www.jneurosci.org) as supplemental material). Another miRNA, miR-128, known to be specifically expressed in neurons (Smirnova et al., 2005), was likewise present in dIP-bodies (Fig. 2B) and also found to be enriched in purified synaptosomes (supplemental Fig. S6B, available at [www.jneurosci.org](http://www.jneurosci.org) as supplemental material). However, it should be noted that *in situ* hybridization also revealed the presence of miRNAs in some foci not overlapping with this P-body marker (Fig. 2A,B), similar to the case of Ago2 (see above).

To find out whether mRNAs repressed by miRNAs were also targeted to dIP-bodies, hypothalamic neurons were transfected with a plasmid expressing a Renilla luciferase (RL) reporter mRNA designed to be translationally repressed by let-7 miRNA, and known to accumulate in P-bodies in HeLa cells (RL-3xB) (Pillai et al., 2005). This mRNA, but not the control reporter mRNA containing mutated let-7 sites, showed colocalization with CFP-Ago2 foci in dendrites, consistent with its enrichment in dIP-bodies (Fig. 2C; supplemental Fig. S6C, available at [www.jneurosci.org](http://www.jneurosci.org) as supplemental material). We have obtained similar results with Dcp1a (data not shown). Thus, similar to the situation observed in somatic cells, dIP-bodies contain miRNAs and mRNAs undergoing miRNA-mediated repression.



### Relationship between dLP-bodies and other RNA granules

Numerous proteins involved in mRNA metabolism were shown to localize to different types of granules in dendrites of neuronal cells (see Introduction), but little is known about how these granules relate to each other and to dLP-bodies. Thus, we compared the localization of three proteins that have been observed to form granules in dendrites, ZBP1, FMRP, and SMN, with the localization of either of Dcp1a or GW182. Their localization in dendrites was further compared with that of the neuronal cell body and HeLa cells.

Antibodies against ZBP1 labeled foci in dendrites of hippocampal and hypothalamic neurons, and a significant fraction of them was stained by antibodies against GW182 or Dcp1a (Fig. 3A and data not shown). The frequency at which ZBP1 was present in dLP-bodies was measured with fluorescent proteins expressed in hypothalamic neurons, using Dcp1a as a reference. We found that 90% ( $\pm 8\%$ ) and 70% ( $\pm 5\%$ ) of CFP-Dcp1a foci contained YFP-ZBP1 in dendrites and soma, respectively. However, similar to the case of Ago2, YFP-ZBP1 was often forming dendritic foci that did not contain detectable Dcp1a (supplemental Fig. S4, available at [www.jneurosci.org](http://www.jneurosci.org) as supplemental material). Interestingly, in HeLa cells, only 24% ( $\pm 6\%$ ) of CFP-Dcp1a foci were positive for YFP-ZBP1 (supplemental Fig. S7, available at [www.jneurosci.org](http://www.jneurosci.org) as supplemental material). Association between ZBP1 and P-body components in neuronal cells was also tested by coimmunoprecipitation experiments, using synaptoneurosomal preparations and antibodies against ZBP1 and RCK/p54 (Fig. 3E). The anti-ZBP1 antibody coimmunoprecipitated RCK/p54 whereas the anti-RCK/p54 immunoprecipitated material was positive for ZBP1, indicating that the colocalization reflected a physical association, either direct or indirect.

We were unable to obtain reliable labeling with anti-SMN and anti-FMRP antibodies in hypothalamic or hippocampal neurons, and we thus used plasmids expressing fluorescently tagged proteins and labeled dLP-bodies with antibodies against Dcp1a. Nearly all Dcp1a foci contained GFP-FMRP, both in dendrites and soma of hypothalamic neurons (90%) (Fig. 3C; supplemental Fig. S4, available at [www.jneurosci.org](http://www.jneurosci.org) as supplemental material), and also in HeLa cells (100%; data not shown). Reciprocally, most GFP-FMRP foci contained Dcp1a, indicating that it is also a good marker of dLP-bodies. In the case of SMN-RFP expressing neurons, most SMN positive foci did not contain Dcp1a (75% of SMN foci).

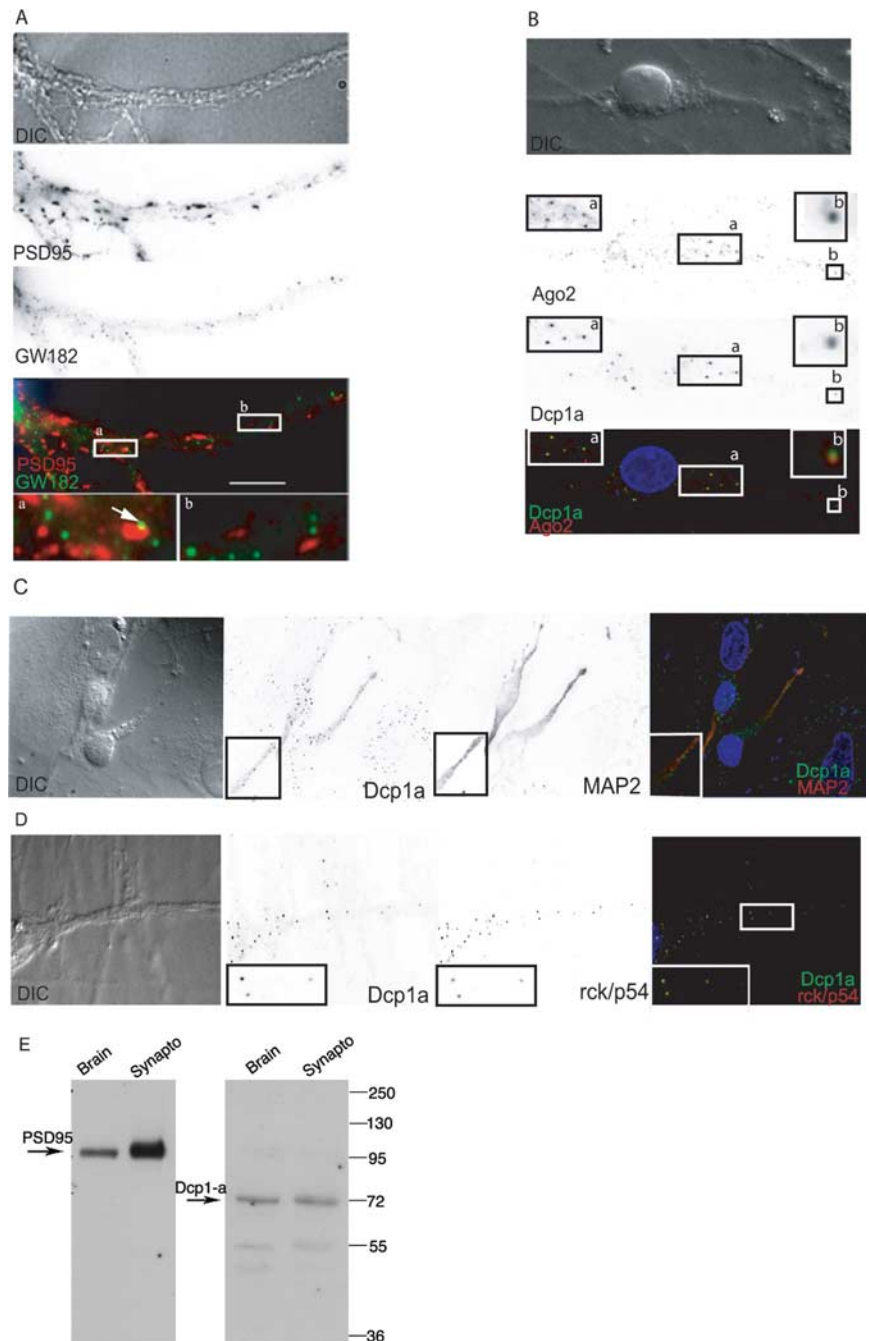
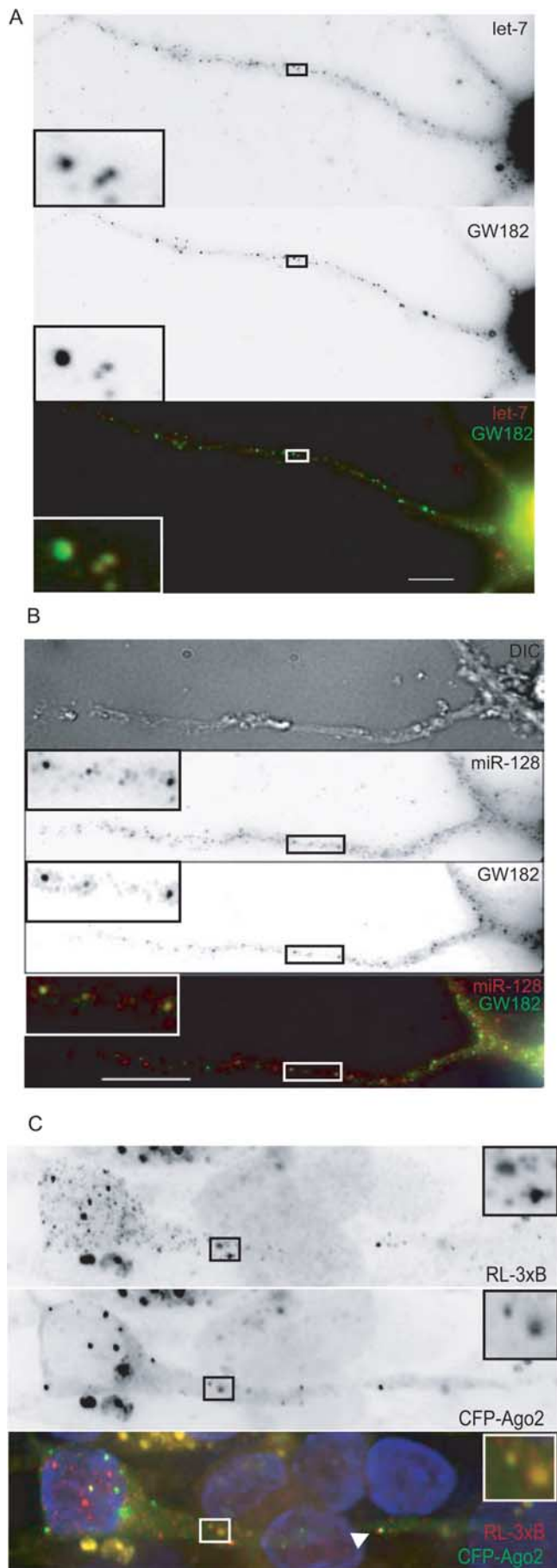


**Figure 1.** *A–E*, Dendritic localization of P-body-like structures in rat hippocampal and hypothalamic neurons. *In vitro* cultured rat hypothalamic (*B–D*) or hippocampal (*A*) neurons were used for immunofluorescence analysis to study the distribution of several P-body markers. In *A–D*, scale bars represent 10  $\mu\text{m}$ . The insets show enlargements of indicated regions (4 $\times$ ). *A*, Costaining of hippocampal neurons with anti-GW182 (bottom) and anti-PSD95 (middle; a marker for synapses) antibodies. GW182-positive granule present close to PSD95 positive synaptic site is marked by an arrow. Overlay (colored panel): GW182 staining is in green and PSD95 in red. DIC image of the same dendrite is shown in the top. *B*, Costaining of hypothalamic neurons with anti-Dcp1a (top) and anti-Ago2 (middle). Overlay (bottom): Dcp1a staining in green, Ago2 in red. *C*, Foci that are stained with anti-Dcp1a serum (left) were also labeled with anti-RCK/p54 antibodies (middle) in processes of cultured hypothalamic neurons. Overlay (right): Dcp1a is in green and rck/p54 is in red. *D*, Anti-Dcp1a antibody (left) labels foci in dendrites of rat hypothalamic neurons. Neurons were costained for neuronal dendritic marker MAP2 (middle). On the overlay (right) panel, Dcp1a is in green and the MAP2 staining is in red. Nuclei are stained with DAPI (in blue). *E*, Western blot reveal the presence of Dcp1a in crude and purified synaptosomal fractions prepared from the mouse brain extract.

Similarly, the fraction of Dcp1a foci that contained SMN was only 30% ( $\pm 10\%$ ) in dendrites and 35% ( $\pm 6\%$ ) in soma (Fig. 3D), whereas no colocalization was observed in HeLa cells (supplemental Fig. S7, available at [www.jneurosci.org](http://www.jneurosci.org) as supplemental ma-



terial). Altogether, these experiments show that dIP-bodies frequently contain ZBP1 and FMRP, and rarely SMN.

Xrn1 has a 5' to 3' exonuclease activity and is an important component of P-bodies of HeLa cells. To find out whether it is also present in P-bodies of hypothalamic neurons, we immunolabeled Dcp1a and Xrn1. As expected, Xrn1 colocalized with Dcp1a in P-bodies of HeLa cells (Fig. 4D). However, the two proteins showed only a partial colocalization in hypothalamic neurons. In the cell body 70% ( $\pm 6\%$ ) of Dcp1a foci contained Xrn1, but in dendrites this was the case for only 10% ( $\pm 5\%$ ) of them. In some cells, Xrn1 appeared to be restricted to the cell body (Fig. 4A).

We also tested for the presence of ribosomes in dIP-bodies, using Y10b antibodies that recognize rRNA. Importantly, staining with this antibody was previously found to be the most conclusive tool to document the presence of ribosomes in neuronal granules (Kim et al., 2005). As expected, there was no detectable accumulation of rRNA in Dcp1a foci in HeLa cells (Fig. 4C). However, rRNA was present in a fraction of dIP-bodies stained by GW182 antibodies in dendrites of hippocampal neurons ( $33 \pm 8\%$ ) (Fig. 4B). In the cell body, the diffused intense staining obtained with Y10B antibody made the assessment of colocalization difficult.

The results described above point to major differences in the composition of P-body-like structures between neuronal processes, neuronal cell body, and HeLa cells. A large fraction of dIP-bodies visualized with anti-Dcp1a or anti-GW182 antibodies lacks Xrn1 but contains ribosomes, and a fraction of previously described neuronal granules containing ZBP1, FMRP may represent dIP-bodies.

#### dIP-bodies display directed movements

To investigate whether dIP-bodies could be involved in transport of mRNAs in dendrites, we assessed whether they were motile by performing video-microscopy of primary hypothalamic neurons expressing GFP-tagged components (Fig. 5 and supplemental Movies 1, 2, 3, available at [www.jneurosci.org](http://www.jneurosci.org) as supplemental material). Indeed, we found that dIP-bodies labeled with GFP-Dcp1a or GFP-Ago2 moved with rectilinear trajectories and at constant velocities, indicating a motor-driven movement. During a 5 min observation period, 26.9% of GFP-Dcp1a foci and 38.6% of Ago2 foci displayed such movements. Detailed analysis of directed movements (supplemental Fig. S8, available at [www.jneurosci.org](http://www.jneurosci.org) as supplemental material) revealed that, for GFP-Dcp1a, 9.7% were retrograde movements, 14.9% anterograde movements, and 2.3% bidirectional. Furthermore, dIP-bodies moved an average distance of 5.4  $\mu\text{m}$  (5.5  $\mu\text{m}$  for anterograde movement, 5.3  $\mu\text{m}$  for retrograde movement), and at an average speed of 0.87  $\mu\text{m}/\text{s}$  (0.75  $\mu\text{m}/\text{s}$  for anterograde, and 0.99  $\mu\text{m}/\text{s}$  for retrograde). The values were similar for GFP-Dcp1a and GFP-Ago2, in agreement with their high degree of colocalization in fixed cells. Together, these data suggest that movements of dIP-bodies depend on active transport, mediated by molecular motors. Interestingly, this property appears to be specific for neurons

←

**Figure 2.** Localization of miRNAs and their mRNA targets in dIP-bodies. **A, B,** Colocalization of miRNAs and GW182 in dIP-bodies of hypothalamic (**A**) and hippocampal (**B**) neurons. miRNAs let-7 (**A**) or miR-128 (**B**) were detected by *in situ* hybridization (top). Staining with anti-GW182 antibody is shown in middle panels. Overlay pictures are shown in bottom, with staining for miRNA in red and for GW182 in green. **C,** Hypothalamic neurons were cotransfected with plasmids expressing CFP-Ago2 (middle) and a *Renilla luciferase* (RL) mRNA reporter with three let-7 binding sites in its 3' UTR (RL-3xB; top). *In situ* hybridization, using probes complementary to RL mRNA, detected the mRNA (red) in foci that are also positive for CFP-Ago2 (green; bottom). Scale bar, 10  $\mu\text{m}$ . The insets show 4 $\times$  enlargements of indicated areas. DAPI was used for staining the nuclei.



since P-bodies of HeLa cells did not show obvious directed movements (data not shown).

Because SMN sometimes colocalized with Dcp1a in dIP-bodies, we also compared the mobility of SMN to that of Dcp1a. As shown in Figure 5, 70.5% of SMN-RFP granules followed a directed movement during a 5 min observation period. Among them, 29.5% showed a retrograde movement, 30.8% an anterograde movement, and 10.26% a bidirectional movement. Generally, SMN-RFP moved over longer distances ( $7.07 \mu\text{m}$  on average) and at a higher velocity ( $1.78 \mu\text{m/s}$  on average) than GFP-Dcp1a and GFP-Ago2. These findings are in agreement with the observations that most SMN granules are distinct from dIP-bodies.

### Synaptic activation relocates dIP-bodies to distant dendritic sites

Having observed the motorized transport of dIP-bodies along dendrites, we wanted to determine whether their localization was modified on synaptic activation. To this end, we measured dendritic distribution of dIP-bodies in hypothalamic neurons that were either untreated or incubated with  $30 \mu\text{M}$  NMDA, a glutamate agonist (Fig. 6*A,B*). Neurons were transfected with GFP-Dcp1a or GFP-Ago2, and we measured in each cell the maximal distance between dIP-bodies and the cell body (Fig. 6*C*, upper graph). We used a software that measured the exact distances in the cell, taking in account the contour of the cellular processes (see Material and Methods). The results indicated that after 5 min of NMDA treatment, there was no significant change (maximal distance of  $72 \pm 9 \mu\text{m}$ , compared with  $62 \pm 7 \mu\text{m}$  for untreated cells). In contrast, after the 15 min treatment, dIP-bodies were localizing as far as  $240 \pm 20 \mu\text{m}$  away from the soma. To obtain a more general view of the localization of dIP-bodies, we then quantified the distribution of GFP-Ago2 positive foci along dendrites, using  $50 \mu\text{m}$  slices from the cell body (Fig. 6*D*). In cells treated with NMDA for 15 min, the distribution of dIP-bodies shifted to distal regions: 50% were distributed  $100$ – $250 \mu\text{m}$  away from the soma, compared with 10% in control cells. This indicates that dIP-bodies respond to synaptic activation by re-localizing to more distant sites in dendrites.

To better characterize which glutamate receptor was involved in the re-localization of dIP-bodies, we treated cells with different drugs that stimulated either ionotropic (kainate) or metabotropic receptors (DHPG), and we measured the distance from the soma of the most distal granule, as described above. DIP-bodies relocated to distal ends of the cell after treatment with kainate,

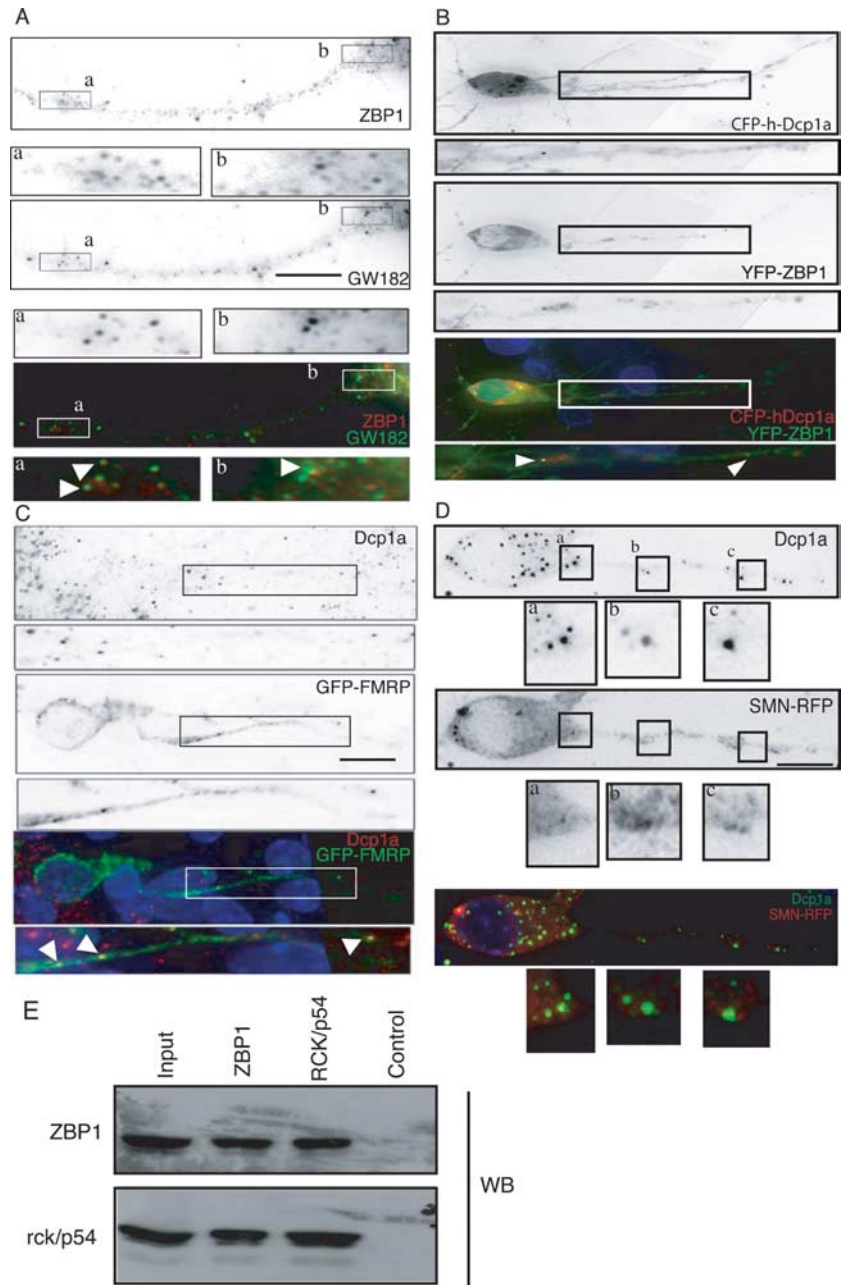


**Figure 3.** dIP-bodies contain translational repressor proteins. **A**, Anti-ZBP1 (top) and anti-GW182 (middle) antibody were used for detection of endogenous proteins in hippocampal neurons. On the overlay (bottom) panel, ZBP1 is in red, and GW182 in green. Colocalizations in panel (**A–D**) are marked by arrowheads. Scale bars,  $10 \mu\text{m}$ . The insets show  $4\times$  enlargements of indicated regions. DAPI was used for staining the nuclei. **B**, Hypothalamic neurons transfected with CFP-Dcp1a (top) and YFP-ZBP1 (middle) show colocalization of CFP and YFP signals in discrete foci. Overlay (lower) panel shows colocalization of CFP-Dcp1a (red) with YFP-ZBP1 (green). **C**, GFP-tagged FMRP (middle) colocalizes with the endogenous Dcp1a (top) in dIP-bodies of hypothalamic neurons transfected with the GFP-FMRP expression plasmid. Overlay (bottom) panel shows colocalization of Dcp1a (red) with GFP-FMRP (green). **D**, Localization of SMN and Dcp1a proteins in hypothalamic neurons. Neurons expressing SMN-RFP (middle) were labeled with anti-Dcp1a (top). In overlay panel (bottom) Dcp1a is in green and SMN-RFP in red. **E**, ZBP1 and RCK/p54 coimmunoprecipitate with each other in protein extracts prepared from purified synaptosomes. Input represents 10% of the total extract used for each immunoprecipitation reaction. Rabbit polyclonal antibody against GRP78 protein was used in control immunoprecipitation.

whereas DHPG had little or no effect (Fig. 6*E*). Furthermore, antagonists of kainate and NMDA, such as DNQX and MK801, blocked the relocalization of dIP-bodies, whereas treatment with MK801 or DNQX alone had no effect. Interestingly, both BDNF and KCl treatments also caused the relocalization of dIP-bodies to distant sites in dendrites (Fig. 6*E*).

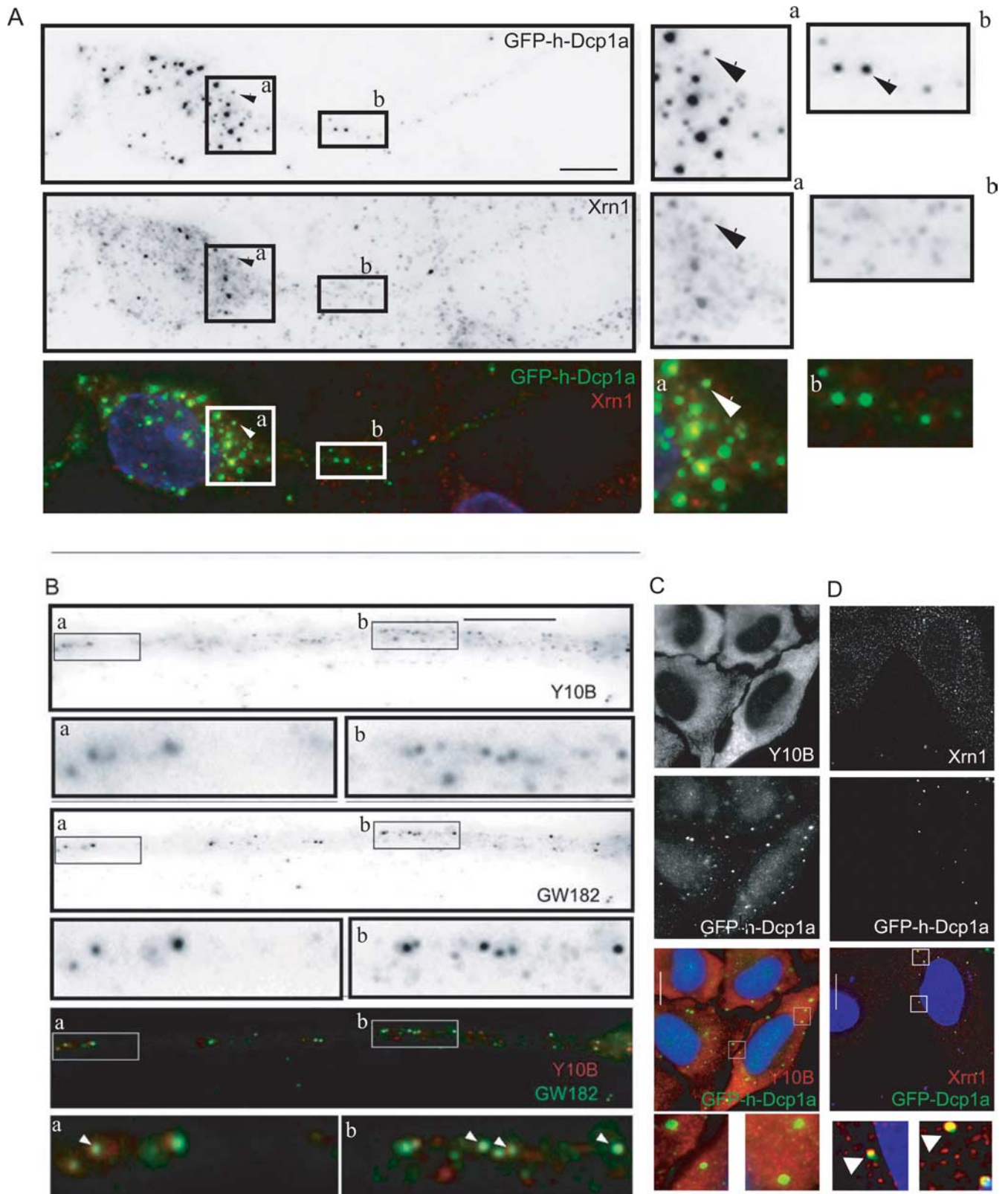


**Figure 4.** dLP-bodies rarely contain the exonuclease Xrn1, but contain rRNA. **A**, Localization of Xrn1 (middle panel) and Dcp1a (top) in hypothalamic neurons transfected with a GFP-Dcp1a expression plasmid. The overlay (bottom) shows Xrn1 staining in red, GFP-Dcp1a in green and nuclei, stained with DAPI, in blue. A rabbit anti-Xrn1 antibody was used for detection of endogenous Xrn1. Insets (2x enlargements) show localization of both proteins in soma (left insets) and dendrites (right insets). **B**, Colocalization of rRNA (staining with Y10B mAb in top; red signal in the overlay panel) with anti-GW182 antibodies (middle; green in the overlay) in hippocampal neurons. Insets show 4x enlargements of the selected areas. **C, D**, Localization of rRNA (**C**) or Xrn1 (**D**) in HeLa cells (top; red in the overlay panel) transfected with GFP-Dcp1a (middle panels; green in the overlay). Nuclei are stained with DAPI (blue in the overlay). Scale bars: 10  $\mu$ m (in **A, B**); 5  $\mu$ m (in **C, D**).

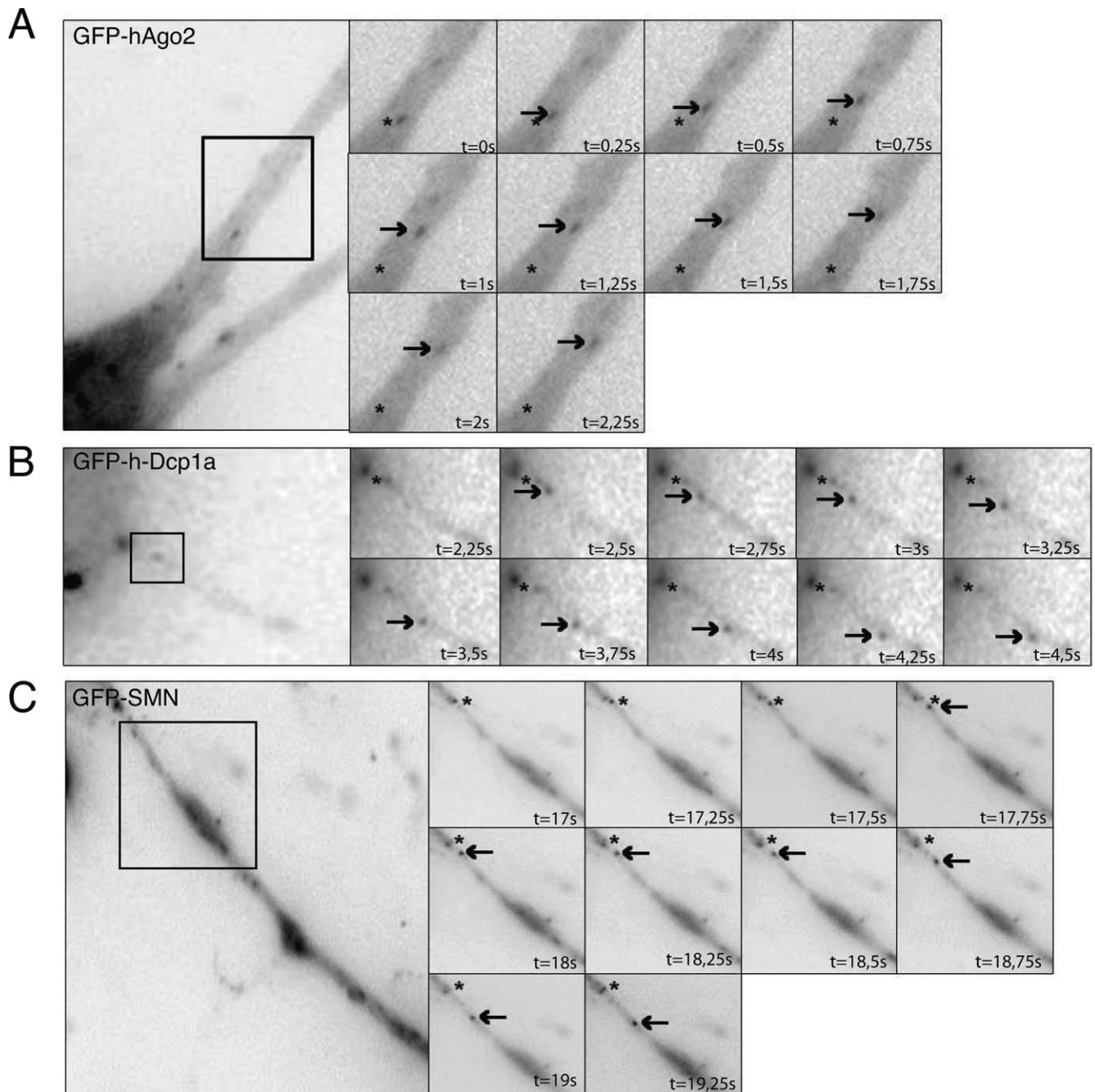


**Figure 5.** P-body components show directed and motorized movements along dendrites of rat neurons. Hypothalamic neurons transfected with GFP-Ago2 (**A**), GFP-Dcp1a (**B**) or GFP-SMN (**C**) were analyzed by time-lapse microscopy. Insets show enlargements ( $5\times$  for GFP-Ago2,  $60\times$  for GFP-Dcp1a, and  $11\times$  for GFP-SMN) of pictures taken at 250 ms intervals. Asterisks indicate initial position of foci, and arrows indicate their position at the indicated time.

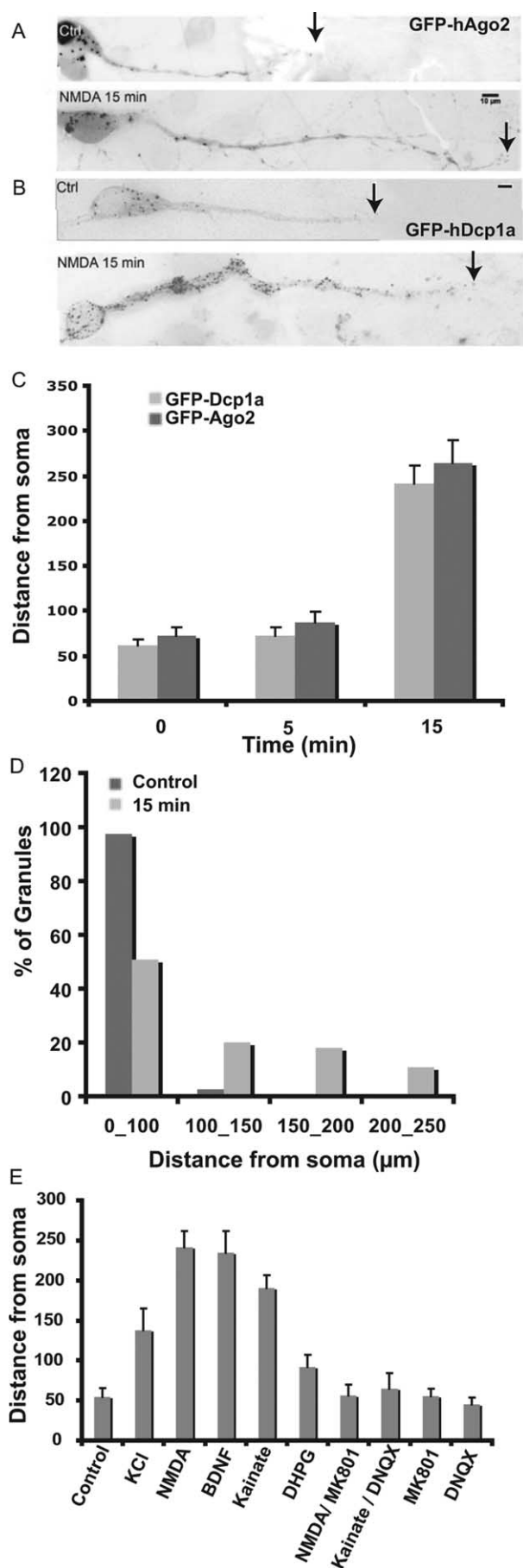
### Synaptic activation stimulates the exchange of P-body components

Although the above experiments analyzed the properties of dIP-bodies as a single entity, they provide little information on the rate of exchange of the dIP-body components with the surrounding cytosol. This is however an important point as a storage function would imply long residency times of dIP-body constituents. To address this question, we performed FRAP analysis on GFP-Dcp1a and GFP-Ago2 positive foci, both in dendrites and soma of hypothalamic neurons, and in HeLa cells. Individual bodies were bleached and fluorescence recovery was recorded during at least 15 min. Because dIP-bodies may move during this time, we used a 3D tracking algorithm that precisely measured the fluorescent

signal within the foci (see Material and Methods). As shown in Figure 7B–D, GFP-Dcp1a was exchanged slowly from foci of hypothalamic neurons, with an immobile fraction of 92% in the cell body and 90% in dendrites. GFP-Ago2 had also a large immobile fraction in neurons, of 80% in both soma and dendrites (Fig. 7F–H). In HeLa cells, the exchange rate of GFP-Ago2 (Fig. 7E) was similar, with an immobile fraction of  $\sim 75\%$ . In contrast, GFP-Dcp1a was much more dynamic, as most of the signal was recovered within few minutes, with an immobile fraction of only 20% after 15 min. Altogether, these data indicate that GFP-Dcp1a is stably associated with dIP-bodies of hypothalamic neurons, but is rapidly exchanged in P-bodies of HeLa cells.

Because synaptic activation had a strong effect on the localiza-





tion of dIP-bodies, it was possible that it could also modify the dynamic properties of their constituents, eventually leading to a modification of their composition. To this end, we repeated the FRAP experiments after synaptic activation. Remarkably, in hypothalamic neurons treated with 30 μM NMDA for 15 min, GFP-Dcp1a exchanged quickly from dIP-bodies, with a turn-over rate similar to P-bodies in HeLa cells (Fig. 7G). To test whether the composition of dIP-bodies may be modified during the course of neuronal activation, we performed double-staining experiments using antibodies against endogenous Dcp1a and Ago2. Whereas in untreated cells nearly all Dcp1a foci contained Ago2 (Figs. 1, 7H), the situation had dramatically changed on synaptic activation: approximately half of the Dcp1a foci did not stain for Ago2 (56 ± 10% and 45 ± 6%, after 15 and 60 min of treatment with 30 μM NMDA, respectively) (Fig. 7J,K).

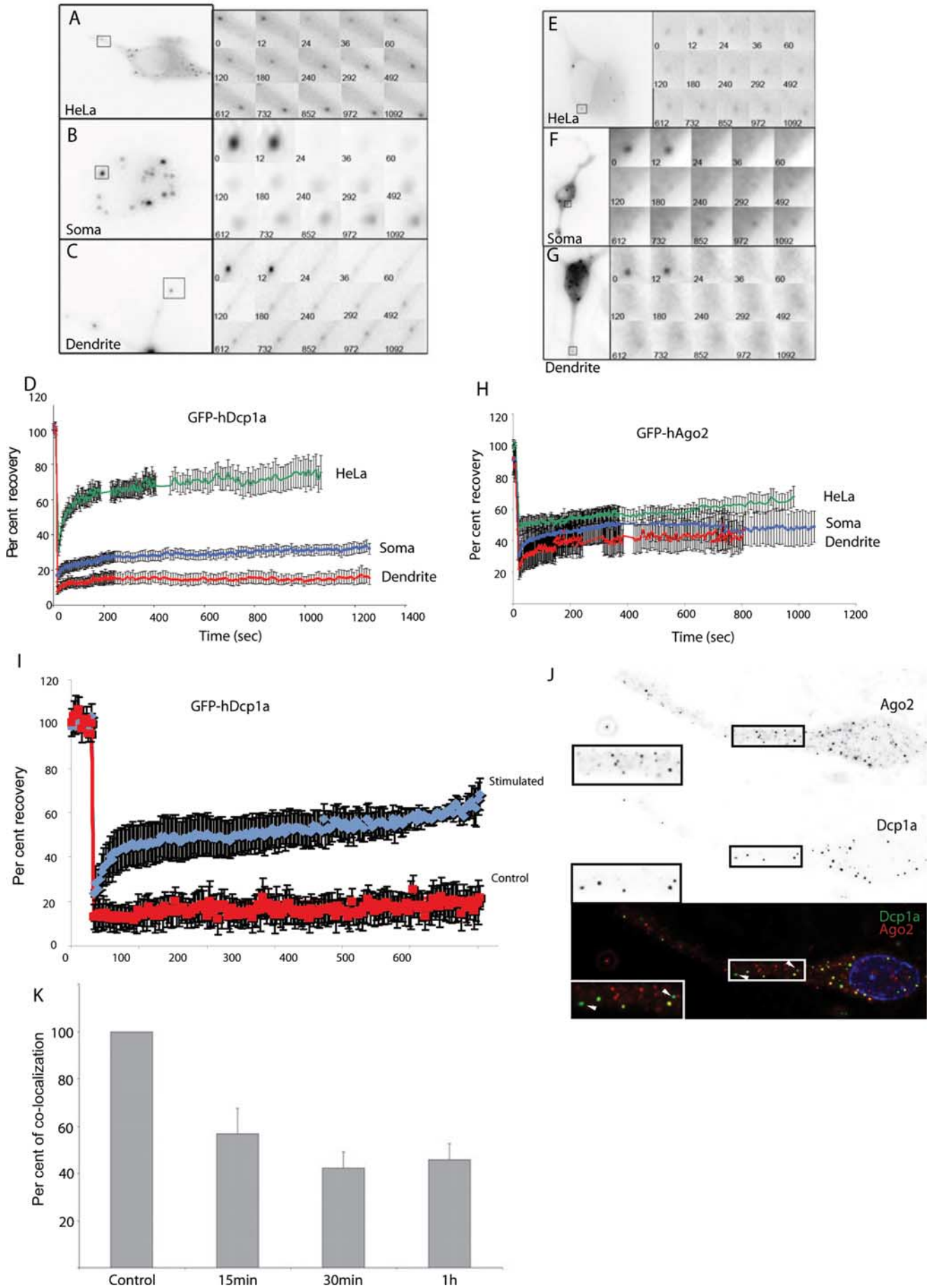
### Discussion

P-bodies have recently emerged as structures implicated in mRNA catabolism and storage, and also in the regulation of mRNA stability and translation by miRNAs (Parker and Sheth, 2007; Pillai et al., 2007). In mammals, most studies have addressed the function of P-bodies in nonpolarized cell lines, with not much attention paid to the role of these structures in neurons, and to their potential relationship to other neuronal granules implicated in transport and storage of mRNAs (Kiebler and Bassell, 2006). In this study, we characterized a novel structure, termed dIP-bodies, which contains many P-body components such as Dcp1a, GW182, and RCK/p54. DIP-bodies are present in the cell body and dendrites of rat hippocampal and hypothalamic neurons, whereas no foci positive for Dcp1a were identified in axons.

Unexpectedly, a large fraction of dIP-bodies was also found enriched in ZBP1 and FMRP, two proteins previously implicated in translational repression and transport of mRNAs in neuronal processes. Our results are consistent with a recent report showing that in *Drosophila* neurons, mRNP granules positive for Staufen and the FMRP-related protein, dFMRP, also contain P-bodies proteins, including homologs of Xrn1, Dcp1a, RCK/p54 (Me31B), and an Argonaute protein Ago2. In addition, it was demonstrated that Me31B and TraI function in a complex with dFMRP and regulate dendrite morphogenesis in *Drosophila* sensory neurons (Barbee et al., 2006). Altogether, these results indicate that at least some mRNP granules present in processes of both mammals and *Drosophila* neurons may correspond to a specialized class of P-bodies, adapted to neuronal function. Interestingly, the partial colocalization observed for many investigated proteins points toward heterogeneity of neuronal P-bodies and other granules.

Both ZBP1 and FMRP have been implicated in transport of specific mRNAs to synapses (Zhang et al., 2001; De Diego Otero

**Figure 6.** *A, B*, Treatment with NMDA and other synaptic activators relocates dIP-bodies to distant parts of dendrites of rat neuron. Localization of GFP-Ago2 (*A*) and GFP-Dcp1a (*B*) positive foci in hypothalamic neurons either untreated (Ctrl) or after 15 min treatment with 30 μM NMDA. *C*, Quantification of the distance between dIP-bodies and the cell body. GFP-Ago2 (dark gray) and GFP-Dcp1a (light gray) in untreated neurons and in neurons treated with NMDA for 5 or 15 min. The numbers represent the maximum distance from cell soma in which GFP-Ago2 or GFP-Dcp1a foci were detectable. *D*, Distribution of GFP-Ago2 positive foci along dendrites before and after 15 min NMDA treatment (*n* = 11). *E*, Quantification of dendritic distribution of GFP-Dcp1a after 15 min treatment with different glutamatergic receptor agonists: NMDA (30 μM), kainate (50 μM) or DHPG (50 μM), or BDNF (50 mg/ml) and KCl (50 mM). When indicated, specific antagonists of NMDA and kainate, MK-801 (10 μM) and DNQX (50 μM), respectively, were added to the culture medium. The numbers the maximum distance from cell soma in which GFP-Ago2 or GFP-Dcp1a foci were detectable after different treatments (*n* = 14).



et al., 2002; Tiruchinapalli et al., 2003; Rackham and Brown, 2004; Antar et al., 2005; Zalfa et al., 2006), and our observations that these proteins associate with dIP-bodies suggest that these structures may be involved in mRNA transport. Indeed, we showed by time-lapse microscopy experiments that whereas P-bodies of HeLa cells show random cytoplasmic movements, dendritic dIP-bodies marked with GFP-Dcp1a or GFP-Ago2 move bidirectionally along rectilinear trajectories, and at constant velocities. Our data are in agreement with the measurements made for ZBP1 (Tiruchinapalli et al., 2003), which, as shown in our study, is a component of the neuronal dIP-bodies. Similarly, dFMRP has been shown to move bidirectionally with a comparable velocity in *Drosophila* dendrites (Ling et al., 2004). These observations argue that movements of dIP-bodies in dendrites depend on active transport, mediated by molecular motors. Interestingly, we found that SMN moves over longer distances with a higher velocity. It has been reported that members of dynein and kinesin superfamily of motor proteins show a wide range of velocity (Hirokawa, 1998). Thus, movement of dIP-bodies could involve motors which are different from those used by SMN granules and further work will be necessary to identify specific motors involved in transport of these different structures.

In agreement with a role of neuronal dIP-bodies in mRNP transport, we found that treatment of cultured rat neurons with NMDA re-localized them to more distant sites in dendrites. It has previously been shown that mobility of dendritic ZBP1 granules colocalizing with  $\beta$ -actin mRNA or ZBP1 alone changes in response to KCl-induced depolarization or NMDA receptor blockage (Tiruchinapalli et al., 2003). However, it is presently unclear whether the increased transport is specifically oriented toward activated synaptic structures or just represents a general enhancement of granule trafficking along the dendrites in response to stimulation. Interestingly, by using different synaptic activators, we observed that dIP-bodies responded to ionotropic glutamate receptors. Moreover, BDNF and KCl also induced re-localization of dIP-bodies, suggesting that they respond to a number of different synaptic stimulations.

Many mRNPs are transported in a translationally silent form. We found that most dIP-bodies are deficient for exonuclease Xrn1, but contain rRNA, a ribosomal component, suggesting a primarily storage function of these structures in dendrites, as opposed to a more general catabolic function of P-bodies in the soma. In agreement with this idea, we found in FRAP experiments that even after 15 min, Ago2 remains almost not exchanged from dIP-bodies (immobile fraction of 75–80%). Most significantly, whereas Dcp1a was rapidly exchanged from P-bodies of HeLa cells as previously described (Leung et al., 2006), we found that it turned-over slowly in dIP-bodies (immobile fraction of 90% after 15 min). Slow exchange of their components indicates that neuronal dIP-bodies, unlike P-bodies in other cell types, represent stable structures, consistent with the idea that they are involved in mRNP storage rather than degradation.

←

**Figure 7.** Synaptic stimulation modifies the exchange rates of dIP-bodies components and modifies their composition. Hypothalamic neurons and HeLa cells expressing GFP-hDcp1a (**A–C**) or GFP-Ago2 (**E–G**) were analyzed by FRAP. Specific foci were bleached after 30 s recording, and fluorescent signals were recorded over time. Images of individual cells and enlargement of the bleached foci is shown. The graphs show recovery curves against time for GFP-hDcp1a foci (**D**) or Ago2 foci (**H**). **I**, FRAP analysis of GFP-hDcp1 in dendrites before (blue) or after stimulation with 30  $\mu$ M NMDA (red). **J**, Hypothalamic neurons were stimulated (30  $\mu$ M NMDA for 15 min), and analyzed by immunofluorescence with antibodies against Ago2 and hDcp1a. **K**, Quantification of the fraction of Dcp1a foci that contained Ago2.

Recently, Schrott et al. (2006) have shown that in mammalian neurons the miRNA miR-134 plays a role in translational repression of an mRNA encoding the synapse remodeling protein LIMK1. Treatment of cultured neurons with a neurotrophic factor BDNF resulted in increased translation of LIMK1 mRNA at postsynaptic sites, likely because of the partial relief of the miR-134-mediated repression. It is not known how miR134 and LIMK1 mRNA are transported to distal dendritic sites and what is the mechanism underlying the local translational activation of LIMK1 mRNA. In cultured non-neuronal mammalian cells, miRNAs and their repressed mRNA targets are enriched in P-bodies (Pillai et al., 2007). Importantly, the repressed mRNAs stored in P-bodies can be mobilized to enter active translation in response to different cues, as shown for the CAT-1 mRNA, a target of miR-122, in human hepatoma cells (Bhattacharyya et al., 2006). We show here that dIP-bodies in dendrites contain Ago2, miRNAs and are also enriched in a repressed reporter mRNA, targeted by let-7 miRNA. Furthermore, we found that Dcp1a is stably associated to dIP-bodies in unstimulated cell, but exchanges rapidly in and out of dIP-bodies on NMDA treatment. Concomitantly, in our study, the composition of dIP-bodies changes, and many of them loose Ago2, suggesting that they release the miRNA repressed mRNPs. In a recent study (Zeitelhofer et al., 2008), the authors found that hippocampal Dcp1a foci are distinct from staufen transport granules, and that they disassemble on synaptic stimulation. Both studies thus suggest that hypothalamic dIP-bodies or hippocampal dendritic P-bodies undergo profound modification on synaptic stimulation. These considerations, taken together with other properties of dIP-bodies discussed above, make them excellent candidates for structures participating in transport and local regulation of miRNA targets in dendrites of mammalian neurons.

The *cis*-acting sequences important for the localization of dendritic mRNAs are commonly found in their 3'UTRs (Martin and Zukin, 2006). However, for many mRNAs, such targeting sequences have not been identified. We found that translational repression induced by miRNA is sufficient to ensure dendritic localization of a reporter mRNA such as RL-3xB, which lacks any apparent dendritic targeting sequence. Possibly, dendritic transport and localization of some endogenous mRNAs depends on their repression by miRNAs (Ashraf and Kunes, 2006; Kosik, 2006; Schuman et al., 2006). However, if this is indeed the case, additional factors would be needed to determine whether the mRNA is recruited to P-bodies remaining in the soma or into P-body-like structures doomed for dendritic transport. Possibly, translational repression by a miRNA in neuronal soma facilitates mRNA recruitment to P-body-like structure for trafficking to dendrites. How mRNAs in dendrites are reactivated for translation is not clear at present. Cytoplasmic polyadenylation element binding (CPEB) protein or neuron specific ELAV proteins are interesting candidates for factors functioning in the activation process. HuR, a constitutively expressed ELAV protein, has been documented to function in the relief of mRNA from the miRNA-mediated repression and in promoting mRNA exit from P-bodies in somatic cells (Bhattacharyya et al., 2006). It will be interesting to establish whether neuron-specific ELAV proteins, HuB, HuC and HuD, have a similar potential.

## References

- Antar LN, Dichtenberg JB, Plociniak M, Afroz R, Bassell GJ (2005) Localization of FMRP-associated mRNA granules and requirement of microtubules for activity-dependent trafficking in hippocampal neurons. *Genes Brain Behav* 4:350–359.
- Ashraf SI, Kunes S (2006) A trace of silence: memory and microRNA at the synapse. *Curr Opin Neurobiol* 16:535–539.
- Bagni C, Mannucci L, Dotti CG, Amaldi F (2000) Chemical stimulation of



- synaptosomes modulates alpha-Ca<sup>2+</sup>/calmodulin-dependent protein kinase II mRNA association to polysomes. *J Neurosci* 20:RC76:1–6.
- Barbee SA, Estes PS, Cziko AM, Hillebrand J, Luedeman RA, Collier JM, Johnson N, Howlett IC, Geng C, Ueda R, Brand AH, Newbury SF, Wilhelm JE, Levine RB, Nakamura A, Parker R, Ramaswami M (2006) Staufen- and FMRP-containing neuronal RNPs are structurally and functionally related to somatic P bodies. *Neuron* 52:997–1009.
- Bhattacharyya SN, Habermacher R, Martine U, Closs EI, Filipowicz W (2006) Relief of microRNA-mediated translational repression in human cells subjected to stress. *Cell* 125:1111–1124.
- Boireau S, Maiuri P, Basyuk E, de la Mata M, Knezevich A, Pradet-Balade B, BŠcker V, Kornbliht A, Marcello A, Bertrand E (2007) The transcriptional cycle of HIV-1 in real-time and live cells. *J Cell Biol* 179:291–304.
- Cougot N, Babajko S, Seraphin B (2004) Cytoplasmic foci are sites of mRNA decay in human cells. *J Cell Biol* 165:31–40.
- De Diego Otero Y, Severijnen LA, van Cappellen G, Schrier M, Oostra B, Willemsen R (2002) Transport of fragile X mental retardation protein via granules in neurites of PC12 cells. *Mol Cell Biol* 22:8332–8341.
- Deshler JO, Highett MI, Abramson T, Schnapp BJ (1998) A highly conserved RNA-binding protein for cytoplasmic mRNA localization in vertebrates. *Curr Biol* 8:489–496.
- Eom T, Antar LN, Singer RH, Bassell GJ (2003) Localization of a betaactin messenger ribonucleoprotein complex with zipcode-binding protein modulates the density of dendritic filopodia and filopodial synapses. *J Neurosci* 23:10433–10444.
- Eulalio A, Behm-Ansmant I, Izaurralde E (2007) P bodies: at the crossroads of post-transcriptional pathways. *Nat Rev Mol Cell Biol* 8:9–22.
- Fischer M, Kaech S, Knutti D, Matus A (1998) Rapid actin-based plasticity in dendritic spines. *Neuron* 20:847–854.
- Fuchs E, Flugge G, Czech B (2006) Remodeling of neuronal networks by stress. *Front Biosci* 11:2746–2758.
- Havin L, Git A, Elisha Z, Oberman F, Yaniv K, Schwartz SP, Standart N, Yisraeli JK (1998) RNA-binding protein conserved in both microtubule- and microfilament-based RNA localization. *Genes Dev* 12:1593–1598.
- Hirokawa N (1998) Kinesin and dynein superfamily proteins and the mechanism of organelle transport. *Science* 279:519–526.
- Hirokawa N (2006) mRNA transport in dendrites: RNA granules, motors, and tracks. *J Neurosci* 26:7139–7142.
- Kiebler MA, Bassell GJ (2006) Neuronal RNA granules: movers and makers. *Neuron* 51:685–690.
- Kim HK, Kim YB, Kim EG, Schuman E (2005) Measurement of dendritic mRNA transport using ribosomal markers. *Biochem Biophys Res Commun* 328:895–900.
- Kindler S, Wang H, Richter D, Tiedge H (2005) RNA transport and local control of translation. *Annu Rev Cell Dev Biol* 21:223–245.
- Klann E, Dever TE (2004) Biochemical mechanisms for translational regulation in synaptic plasticity. *Nature Rev* 5:931–942.
- Kosik KS (2006) The neuronal microRNA system. *Nat Rev* 7:911–920.
- Krichevsky AM, Kosik KS (2001) Neuronal RNA granules: a link between RNA localization and stimulation-dependent translation. *Neuron* 32:683–696.
- Krichevsky AM, King KS, Donahue CP, Khrapko K, Kosik KS (2003) A microRNA array reveals extensive regulation of microRNAs during brain development. *RNA* 9:1274–1281.
- Lagos-Quintana M, Rauhut R, Yalcin A, Meyer J, Lendeckel W, Tuschl T (2002) Identification of tissue-specific microRNAs from mouse. *Curr Biol* 12:735–739.
- Leung AK, Calabrese JM, Sharp PA (2006) Quantitative analysis of Argonaute protein reveals microRNA-dependent localization to stress granules. *Proc Natl Acad Sci U S A* 103:18125–18130.
- Ling SC, Fahrner PS, Greenough WT, Gelfand VI (2004) Transport of *Drosophila* fragile X mental retardation protein-containing ribonucleoprotein granules by kinesin-1 and cytoplasmic dynein. *Proc Natl Acad Sci U S A* 101:17428–17433.
- Liu J, Valencia-Sanchez MA, Hannon GJ, Parker R (2005) MicroRNA-dependent localization of targeted mRNAs to mammalian P-bodies. *Nat Cell Biol* 7:719–723.
- Martin KC, Zukin RS (2006) RNA trafficking and local protein synthesis in dendrites: an overview. *J Neurosci* 26:7131–7134.
- Meijering E, Jacob M, Sarria JC, Steiner P, Hirling H, Unser M (2004) Design and validation of a tool for neurite tracing and analysis in fluorescence microscopy images. *Cytometry A* 58:167–176.
- Parker R, Sheth U (2007) P bodies and the control of mRNA translation and degradation. *Mol Cell* 25:635–646.
- Pillai RS, Bhattacharyya SN, Artus CG, Zoller T, Cougot N, Basyuk E, Bertrand E, Filipowicz W (2005) Inhibition of translational initiation by Let-7 MicroRNA in human cells. *Science* 309:1573–1576.
- Pillai RS, Bhattacharyya SN, Filipowicz W (2007) Repression of protein synthesis by miRNAs: how many mechanisms? *Trends Cell Biol* 17:118–126.
- Rackham O, Brown CM (2004) Visualization of RNA-protein interactions in living cells: FMRP and IMP1 interact on mRNAs. *EMBO J* 23:3346–3355.
- Rage F, Riteau B, Alonso G, Tapia-Arancibia L (1999) Brain-derived neurotrophic factor and neurotrophin-3 enhance somatostatin gene expression through a likely direct effect on hypothalamic somatostatin neurons. *Endocrinology* 140:909–916.
- Ross AF, Oleynikov Y, Kislauskis EH, Taneja KL, Singer RH (1997) Characterization of a beta-actin mRNA zipcode-binding protein. *Mol Cell Biol* 17:2158–2165.
- Scarborough DE, Scarborough DE, Lee SL, Dinarello CA, Reichlin S (1989) Interleukin-1 beta stimulates somatostatin biosynthesis in primary cultures of fetal rat brain. *Endocrinology* 124:549–551.
- Schratt GM, Tuebing F, Nigh EA, Kane CG, Sabatini ME, Kiebler M, Greenberg ME (2006) A brain-specific microRNA regulates dendritic spine development. *Nature* 439:283–289.
- Schuman EM, Dynes JL, Steward O (2006) Synaptic regulation of translation of dendritic mRNAs. *J Neurosci* 26:7143–7146.
- Smirnova L, Grafe A, Seiler A, Schumacher S, Nitsch R, Wulczyn FG (2005) Regulation of miRNA expression during neural cell specification. *Eur J Neurosci* 21:1469–1477.
- Sutton MA, Schuman EM (2006) Dendritic protein synthesis, synaptic plasticity, and memory. *Cell* 127:49–58.
- Tiruchinapalli DM, Oleynikov Y, Kelic S, Shenoy SM, Hartley A, Stanton PK, Singer RH, Bassell GJ (2003) Activity-dependent trafficking and dynamic localization of zipcode binding protein 1 and beta-actin mRNA in dendrites and spines of hippocampal neurons. *J Neurosci* 23:3251–3261.
- Twiss JL, van Minnen J (2006) New insights into neuronal regeneration: the role of axonal protein synthesis in pathfinding and axonal extension. *J Neurotrauma* 23:295–308.
- van Dijk E, Cougot N, Meyer S, Babajko S, Wahle E, Seraphin B (2002) Human Dcp2: a catalytically active mRNA decapping enzyme located in specific cytoplasmic structures. *EMBO J* 21:6915–6924.
- Xia Z, Dudek H, Miranti CK, Greenberg ME (1996) Calcium influx via the NMDA receptor induces immediate early gene transcription by a MAP kinase/ERK-dependent mechanism. *J Neurosci* 16:5425–5436.
- Zalfa F, Achsel T, Bagni C (2006) mRNPs, polysomes or granules: FMRP in neuronal protein synthesis. *Curr Opin Neurobiol* 16:265–269.
- Zeitelhofer M, Karra D, Macchi P, Tolino M, Thomas S, Schwarz M, Kiebler M, Dahm R (2008) Dynamic interaction between P-bodies and transport ribonucleoprotein particles in dendrites of mature hippocampal neurons. *J Neurosci* 28:7555–7562.
- Zhang HL, Eom T, Oleynikov Y, Shenoy SM, Liebelt DA, Dichtenberg JB, Singer RH, Bassell GJ (2001) Neurotrophin-induced transport of a beta-actin mRNA complex increases beta-actin levels and stimulates growth cone motility. *Neuron* 31:261–275.